water

MDPI

Article

Coupling Iron Coagulation and Microalgal–Bacterial Granular Sludge for Efficient Treatment of Municipal Wastewater: A Proof–of–Concept Study

Bingheng Chen [1], Chenyu Wang [1], Changqing Chen [1], Anjie Li [2], Xiaoyuan Zhang [3], Shulian Wang [4] and Bin Ji [1,5,*]

[1] Department of Water and Wastewater Engineering, School of Urban Construction, Wuhan University of Science and Technology, Wuhan 430065, China; chenbingheng@wust.edu.cn (B.C.); chenyuwang@wust.edu.cn (C.W.); ccq18039301180@wust.edu.cn (C.C.)
[2] Key Laboratory of Water and Sediment Sciences of Ministry of Education, State Key Laboratory of Water Environment Simulation, School of Environment, Beijing Normal University, Beijing 100875, China; liaj@bnu.edu.cn
[3] College of Environmental Science and Engineering, Nankai University, Tianjin 300350, China; zhangxiaoyuan@nankai.edu.cn
[4] Engineering Laboratory of Low-Carbon Unconventional Water Resources Utilization and Water Quality Assurance, College of Environmental Science and Engineering, Nankai University, Tianjin 300350, China; wangshulian@hbut.edu.cn
[5] Hubei Provincial Engineering Research Center of Urban Regeneration, Wuhan University of Science and Technology, Wuhan 430065, China
* Correspondence: binji@wust.edu.cn

Abstract: The rapid expansion of global urbanization and industrialization has significantly increased the discharge of municipal wastewater, leading to issues of carbon emissions and energy consumption when using traditional biological treatment processes. This study proposes an innovative process that couples iron coagulation with microalgal–bacterial granular sludge (MBGS), with optimization and regulation based on operational conditions. The study found that the coagulation performance achieved optimal levels at an iron concentration of 25 mg/L and an anionic polyacrylamide concentration of 1 mg/L, which could remove approximately 61% of the organics and over 90% of phosphorus from raw wastewater. By relying on heterotrophic microorganisms, such as *Proteobacteria*, *Bacteroidota*, and *Chloroflexi*, along with the synergistic interaction between algae and bacteria, the subsequent MBGS process could further effectively remove organics over the day-night cycles. Moreover, the addition of inorganic carbon sources of $NaHCO_3$ increased the abundance of denitrification-related genes, reduced the accumulation of nitrite within MBGS, and led to effective total nitrogen removal. These results indicate that the iron coagulation–MBGS coupling process can efficiently treat municipal wastewater, offering potential for environment-sustainable pollutant removal with reduced energy consumption. These findings provide valuable insights for the practical engineering application of MBGS in wastewater treatment systems aiming for carbon-neutral wastewater treatment.

Keywords: wastewater treatment; emerging pollutants; microbial community; functional genes; carbon neutrality

check for updates

Citation: Chen, B.; Wang, C.; Chen, C.; Li, A.; Zhang, X.; Wang, S.; Ji, B. Coupling Iron Coagulation and Microalgal–Bacterial Granular Sludge for Efficient Treatment of Municipal Wastewater: A Proof–of–Concept Study. *Water* **2024**, *16*, 3035. https://doi.org/10.3390/w16213035

Academic Editor: Andrea G. Capodaglio

Received: 19 September 2024
Revised: 9 October 2024
Accepted: 14 October 2024
Published: 23 October 2024

Copyright: © 2024 by the authors. Licensee MDPI, Basel, Switzerland. This article is an open access article distributed under the terms and conditions of the Creative Commons Attribution (CC BY) license (https://creativecommons.org/licenses/by/4.0/).

1. Introduction

With the rapid acceleration of global urbanization and industrialization, industries such as food processing, catering, slaughterhouses, and dairy production have expanded significantly, leading to a yearly increase in wastewater discharge from these industries [1–3]. This presents significant challenges for wastewater treatment plants in some regions, especially in certain areas of developing countries, because a considerable portion of this type of wastewater ultimately ends up in municipal wastewater treatment plants in these regions. Notably, municipal wastewater in these regions is characterized by a higher

chemical oxygen demand (COD), typically containing high concentrations of phosphorus, fats, and suspended solids, posing significant challenges to wastewater treatment plants [4]. Similarly, urban wastewater treatment plants in high-latitude regions, as well as those in severely water-scarce areas, also face this problem. This municipal wastewater is difficult to biodegrade directly and requires substantial dissolved oxygen (DO) for biodegradation, increasing energy demands for aeration [5]. Additionally, elevated concentrations of phosphorus and suspended solids can impair sludge floc formation, making it difficult for sludge to settle and separate, often resulting in sludge bulking [6]. Furthermore, emerging pollutants in wastewater, such as antibiotics, food additives, and surfactants, may inhibit microbial activity, indirectly affecting the stability of biological treatment systems [7]. A higher COD concentration can also lead to overloading of wastewater treatment facilities, reducing equipment lifespan. In summary, conventional aerobic biological treatment processes are insufficient for treating this type of municipal wastewater. Direct biological treatment could result in high operational and maintenance costs, as well as suboptimal outcomes. Therefore, pretreatment before entering wastewater treatment plants is essential.

Coagulation is an effective pretreatment for municipal wastewater. Iron-based coagulants are particularly useful due to their excellent flocculation properties, which remove suspended solids and organic matter by forming insoluble precipitates, such as iron phosphate [8]. Iron coagulants like ferric chloride ($FeCl_3$) and ferric sulfate ($Fe_2(SO_4)_3$) can hydrolyze to form positively charged hydroxides, neutralizing negatively charged surfactants and emulsified particles. In addition, the sedimentation after coagulation can be used for resource recovery. However, several problems are difficult to address when using iron coagulation for pretreatment and subsequently applying the conventional activated sludge (CAS) process for secondary biological treatment. Firstly, the additional pretreatment step increases the overall carbon footprint of the system (due to reagent addition, mechanical stirring, etc.). Secondly, the accumulation of residual iron ions post-coagulation may be toxic to the sludge [9]. Additionally, the reduced phosphorus content after coagulation may disrupt the nutrient balance, potentially leading to sludge bulking. Therefore, there is a need to develop an energy-efficient secondary biological treatment process that can be coupled with coagulation pretreatment to efficiently treat municipal wastewater.

As an emerging process, microalgal–bacterial granular sludge (MBGS) is gaining recognition as a suitable candidate for wastewater treatment processes after iron coagulation pretreatment. MBGS relies on the symbiotic relationship between microalgae and bacteria, where the microalgae efficiently assimilate carbon dioxide and nutrients, producing oxygen for bacteria to utilize to oxidize organic matter, generating carbon dioxide [10]. This process enables effective pollutant removal with low energy consumption. Compared to activated sludge, MBGS exhibits superior nitrogen and phosphorus removal capabilities due to the synergistic effect of microalgae and bacteria, while retaining the ability to effectively remove various other pollutants. Algae in MBGS can assimilate nutrients such as nitrogen and phosphorus from wastewater, converting them into biomass, which can be further used for biofuel and lipid production, offering potential for resource recovery after wastewater treatment. Thus, the MBGS process appears to be more energy-efficient than the conventional CAS process, significantly reducing the carbon footprint of wastewater treatment systems. Notably, the algae in MBGS may effectively absorb or accumulate iron ions, mitigating the toxic accumulation of iron after coagulation [11]. Moreover, the diverse metabolic pathways and stable granular structure provided by the combination of algae and bacteria give MBGS strong adaptability to external conditions, reducing the risk of sludge bulking to some extent [12]. Previous studies have demonstrated the ability of MBGS to handle a wide variety of wastewaters, such as conventional municipal wastewater, aquaculture wastewater, and wastewater containing emerging contaminants [13]. Research shows that the performance of MBGS could decrease under lower light intensity condition because it relies on photosynthesis to maintain the activity of microalgae, while suspended solids and colored substances in real wastewater significantly reduce light transmittance. However, iron coagulation can remove suspended solids and colored substances, ensuring

that light can reach the MBGS after limited attenuation, thereby enhancing its photosynthetic efficiency. Based on the previous studies mentioned above, MBGS treatment could potentially serve as a suitable secondary biological treatment process when coupled with iron coagulation pretreatment, effectively treating municipal wastewater while alleviating or counteracting the negative effects of coagulation.

Therefore, we developed an iron coagulation–MBGS coupling process for treating municipal wastewater. First, we constructed a complete outdoor reactor system integrating pretreatment and biological secondary treatment and optimized the coagulation pretreatment conditions. We then monitored key water quality indicators and adjusted process parameters accordingly to meet discharge standards. Finally, through experiments, we examined the characteristics of the granule size at various phases, pollutant removal performance, microbial community composition, and metagenomics to assess the feasibility of the coupling process. This study is expected to provide a valuable reference for the practical engineering application of MBGS.

2. Materials and Methods

2.1. Wastewater

Real wastewater was sourced from the canteen sewage system (30°26′42″ N, 114°15′53″ E). $FeCl_3$ was then added, followed by rapid stirring at 300 rpm for 1.5 min using a stirring device [14]. Then, PAM was added as the coagulant aid, followed by slow stirring at 50 rpm for 15 min. After 15 min of sedimentation, the supernatant was collected as the influent for the MBGS bioreactor during phase I (days 1–14) (Figure 1b). The sediment primarily consisted of iron hydroxides, organic matter, and potentially phosphates. The supernatant contained water along with dissolved pollutants, nutrients, and residual iron ions. In phases II and III (days 15–28), based on an empirical formula for algal assimilation of ammonia [10], 0.9 g/L of sodium bicarbonate ($NaHCO_3$) was added to the wastewater as an inorganic carbon source before it entered the reactor. In phase III (days 21–28), while keeping other pollutant concentrations stable, the nitrogen concentration was reduced, doubling the carbon-to-nitrogen ratio of the wastewater.

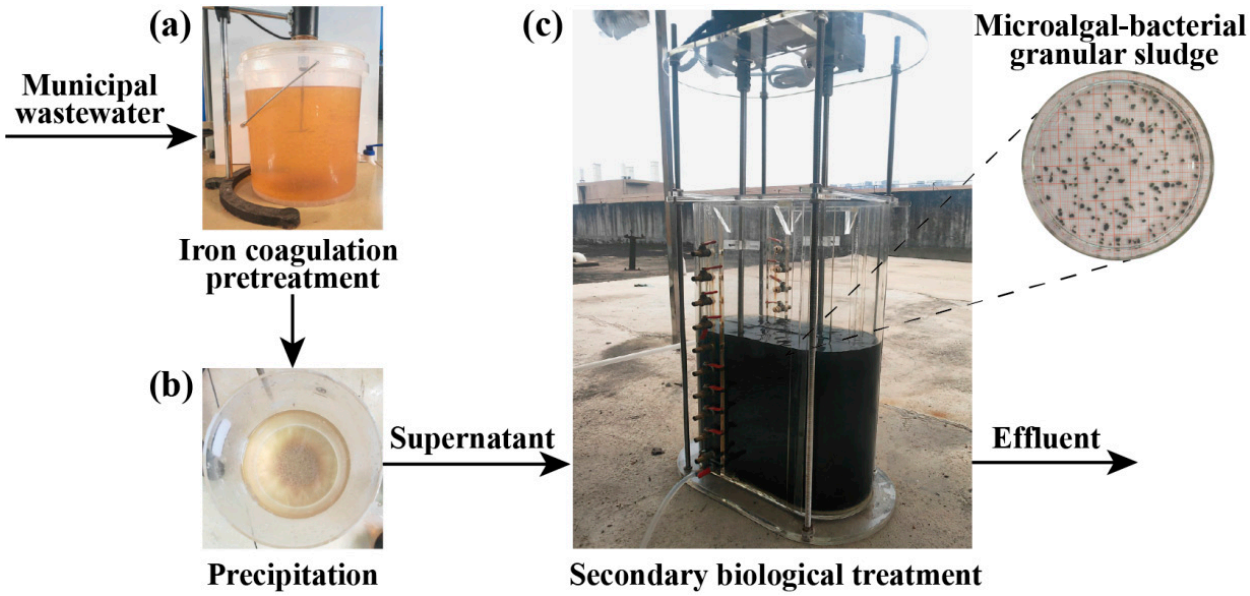


Figure 1. Configuration and composition of MBGS bioreactor: iron coagulation pretreatment (**a**), precipition (**b**), secondary biological treatment (**c**).

2.2. Bioreactor Setup

MBGS was cultivated using previously established methods [15], and, after maturation, the granules were placed into the reactor. The initial average granule size of the MBGS

was approximately 2.3 mm, with a 5 min sludge volume index (SVI_5) of about 39.6 and initial concentrations of volatile suspended solids (VSS) around 2.0 g/L. The bioreactor setup is shown in Figure 1c. The transparent corridor-type reactor had a curved radius and straight length of 8 cm and 20 cm, respectively, with an effective water depth of 35 cm and a total volume of about 18.2 L. The hydraulic retention time (HRT) was set at 12 h. Two stirrers (3RK15RGN-C; Wenzhou Pfeid Mechanical & Electrical Co., Ltd., Wenzhou, China) with a speed of 160 rpm were positioned diagonally near the curved sections of the reactor, 4 cm from the outer wall. Each stirrer was equipped with two four-bladed paddles located 6 cm and 16 cm above the bottom. A peristaltic pump (BT100; Baoding Rongbai Constant-Flow Pump Manufacturing Co., Ltd., Baoding, China) supplied the supernatant after iron coagulation through an inlet at the bottom of the reactor, while an outlet on the opposite upper side collected the effluent. A circular stainless-steel filter with a diameter of 18 mm and a mesh size of 20 was fixed at the outlet of the reactor to prevent the loss of granules. The flow rate of the peristaltic pump was set to 25 ml/min, controlling the hydraulic retention time to approximately 12 h. Effluent samples were collected at sunrise and sunset, filtered through a 0.45 μm membrane, and stored at 4 °C for analysis. During this period, light intensity, dissolved oxygen, and water temperature were measured every 2 h.

2.3. Analytical Methods

The VSS, SVI_5, total nitrogen (TN), total phosphorus (TP), ammonia, and nitrite were measured using standard methods. The turbidity and iron concentration of the wastewater before and after iron coagulation were determined by a portable turbidity meter (WGZ-1B; Hangzhou Qiwei Instrument Co., Ltd., Hangzhou, China) and an inductively coupled plasma-optical emission spectrometer (5110 ICP−OES; Agilent Technologies, Inc., Santa Clara, CA, USA). The granule size was measured using ImageJ 2.0.0 software. The microbial composition and distribution of MBGS under visible light and fluorescence were observed using an inverted fluorescence microscope (Olympus IX83; Tokyo, Japan). The microstructural morphology of MBGS was examined using a scanning electron microscope (SEM) (Gemini 500; Zeiss, Jena, Germany). Chlorophyll, EPS, and glycogen in the sludge were extracted and quantified according to previously established methods [16–18]. The pH and DO were monitored using a pH meter (STARTER3100; Ohaus. Inc., Parsippany, NJ, USA) and an oxygen meter (JPB-607A; INESA Scientific Instrument, Shanghai, China), respectively. The light intensity on the reactor surface was measured using a quantum meter (TES1339P; TES, Taipei, Taiwan, China). Eukaryotic and prokaryotic microbial community analyses were conducted based on the Illumina MiSeq platform. Total genomic DNA was extracted using the E.Z.N.A. Soil DNA Kit (OMEGA Biotek Inc., Norcross, GA, USA) and the FastDNA Spin Kit for Soil (MP Biomedicals, Irvine, CA, USA) for metagenomic sequencing, and metabolic pathways were analyzed using the KEGG and NCyc databases.

3. Results and Discussion

3.1. Iron Coagulation Parameters

An orthogonal experiment was conducted using ferric chloride as the coagulant and PAM as the coagulant aid to investigate the effects of trivalent iron and PAM on the coagulation removal efficiency of pollutants in real wastewater. The coagulation effect was optimal when the concentrations of Fe and PAM were 25 mg/L and 1 mg/L. The turbidity, pH values, and DO before and after coagulation were also measured. The indicators of the wastewater before and after coagulation are shown in Table 1. Anionic polyacrylamide further enhanced the coagulation effect of iron due to its negative charge, which interacts electrostatically with iron ions or particle surfaces, facilitating floc formation [19]. This effective coagulation achieved an organic matter removal efficiency that reached approximately 61%, comparable to the COD levels in typical municipal wastewater (Figure S1). The removal efficiency of total phosphorus exceeded 90%, and turbidity was significantly reduced.

Table 1. The indicators of the wastewater before and after iron coagulation.

Iron Coagulation	Pollutant Concentration (mg/L)							Turbidity (NTU)	DO (mg/L)	pH
	TN	TP	COD	Ammonia	Nitrate	Nitrite	Fe			
Before Coagulation	16–45	3.2–5	500–700	13–35	<0.1	<0.1	<0.1	120–190	3.2–4	7.1–7.5
After Coagulation	15–43	0.05–0.3	140–250	13–34	<0.1	<0.1	0.5–1.2	7–20	5.2–6.5	7.5–7.9

3.2. Pollutant Removal in the Bioreactor

The entire experiment was conducted during the autumn and winter seasons in Wuhan, Hubei Province, under various weather conditions, such as sunny, cloudy, and rainy days. The average light intensity ranged from 65 to 320 μ mol/m^2/s, with average water temperatures between 8 °C and 22.5 °C. Throughout the experimental period, MBGS maintained a relatively stable COD removal efficiency (Figure 2a). Regardless of outdoor conditions, the overall process consistently achieved removal efficiencies of over 86.7% for COD and 95.1% for TP. After appropriate parameter adjustments, the removal efficiencies for TN during the day and night were maintained at approximately 70% and 60%, respectively. Similarly, daytime and nighttime COD removal efficiencies exceeded 81.1% and 71.3%, respectively. This can be attributed to the superior organic matter removal capacity of MBGS, the synergistic interaction between algae and bacteria under light conditions further enhancing the efficient degradation of organic pollutants [10]. From days 1 to 14 (phase I), the total nitrogen removal efficiency gradually declined (Figure 2b), likely due to the denitrification process requiring electron donors produced from the metabolism of carbon sources [20]. The low concentration of organic matter in the wastewater meant that denitrifying bacteria lacked sufficient carbon sources, resulting in inefficient reduction of nitrate to nitrogen gas, leading to the accumulation of nitrite and a decrease in total nitrogen removal efficiency. The concentration of nitrite in the effluent was lower at night (Figure S2), possibly because algae do not perform photosynthesis at night, which limits the aerobic conditions needed for the conversion of ammonia to nitrite. Studies have reported that the accumulation of nitrite can be toxic to microorganisms, inhibiting the nitrifying ability of bacteria to convert ammonia into nitrite [21]. After attempting to supplement the reactor with $NaHCO_3$ as an inorganic carbon source, both the total nitrogen and COD removal efficiencies improved (Figure 2a,b). This is likely because $NaHCO_3$ can be absorbed by algae and used in photosynthesis, thereby enhancing the algae nitrogen assimilation and balancing the demand for limited organic carbon between microalgae and bacteria. Additionally, although $NaHCO_3$ cannot be directly utilized by denitrifying bacteria, it can indirectly promote denitrification by adjusting the carbon source balance in the system. After reducing the influent nitrogen concentration to improve the carbon-to-nitrogen ratio, the total nitrogen removal efficiency increased further, indicating that carbon source deficiency was a key factor in the earlier phases of the experiment. Notably, MBGS demonstrated the ability to further remove low concentrations of phosphorus remaining in the wastewater post-coagulation, particularly under light conditions, due to its capability for advanced treatment and phosphorus assimilation [22]. However, from day 12 onward, the MBGS reactor began releasing phosphorus at night, likely due to polyphosphate-accumulating organisms releasing stored phosphorus under anaerobic conditions (Figure 2c). Additionally, the metabolic shift in algae at night, where they break down phosphate compounds to release energy, contributed to the phosphorus release. In summary, owing to superior pollutant degradation capabilities, the iron coagulation–MBGS coupling process effectively treated wastewater and met discharge standards with appropriate adjustments.

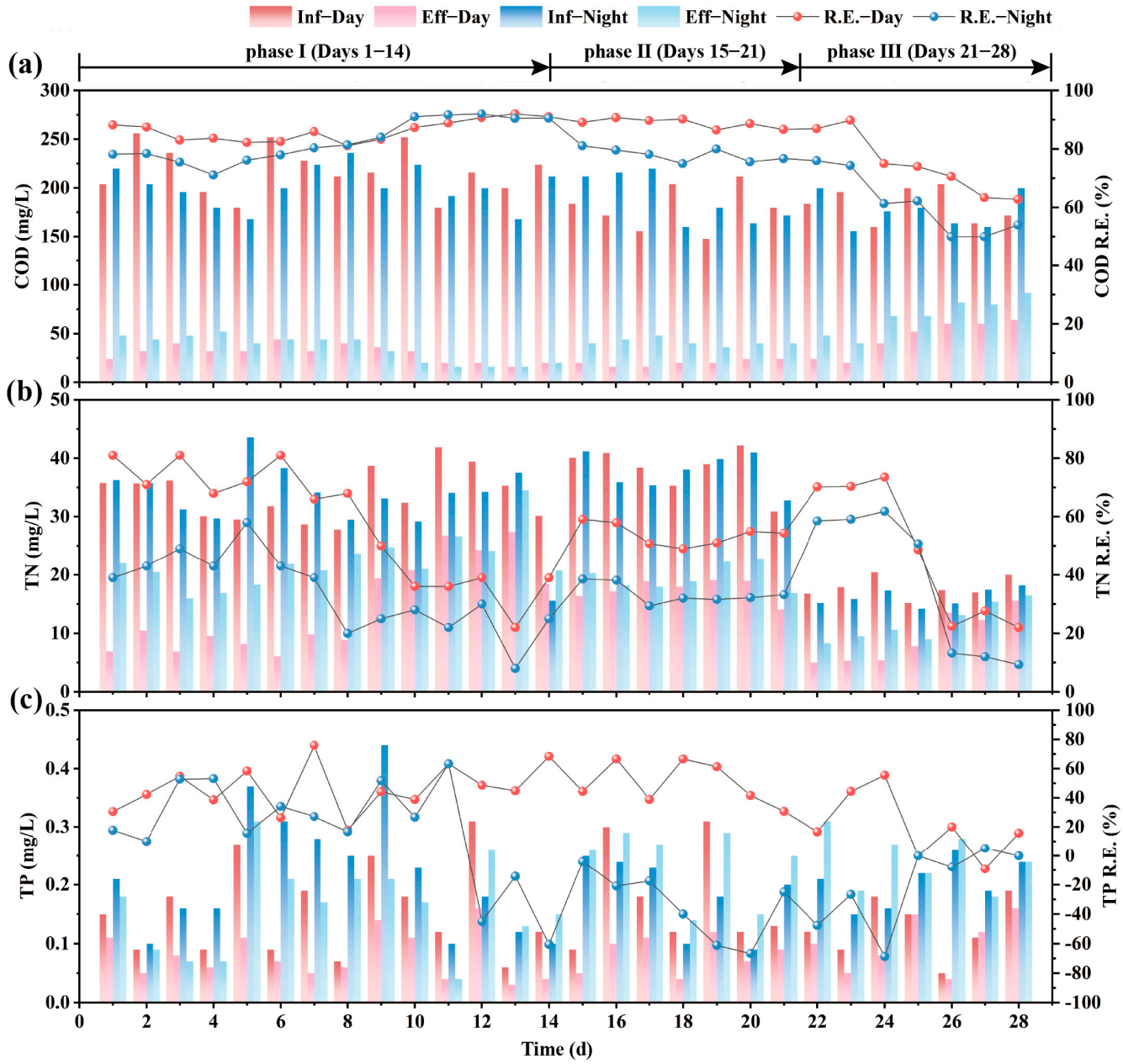


Figure 2. The day and night removal efficiencies and concentrations of COD (**a**), TN (**b**), and TP (**c**) during the iron coagulation–MBGS coupling process.

3.3. Granular Characteristics

Throughout the experimental process, MBGS adapted to the iron coagulation-coupled reaction system by modifying its characteristics. As shown in Figure 3a, the EPS content of the sludge gradually increased over time, likely due to the stress response induced by residual iron and toxic substances, such as detergents from iron coagulation [23]. Microorganisms secrete more EPS to form a protective barrier, a finding confirmed by SEM results (Figure 4). Chlorophyll b also increased during the experiment, possibly due to a higher abundance of *Chlorophyta* and diatoms containing chlorophyll b (Figure 3a). It has been reported that EPS secreted by *Chlorophyta* can enhance iron enrichment by complexing with iron ions [24,25]. The silica-rich structure of *Diatomea* cell walls exhibits strong adsorption capabilities, allowing iron ions to be adhere on the surface and transported into the cells by specific iron transport proteins for photosynthesis and metabolism [26]. At the end of the experiment, the sludge concentration slightly increased (Figure 3b), likely due to the

assimilation of nutrients from the wastewater by microorganisms (including algae and bacteria), leading to a slight increase in overall biomass. However, since organic matter and nutrients in municipal wastewater may be limited, the increase in sludge concentration was relatively slow. Notably, after the experiment, the morphology of the *cyanobacteria* shifted from tightly intertwined straight forms to loose spiral shapes (Figure 4d1–d3), reducing granule density and potentially causing a decline in the sedimentation performance of MBGS. The glycogen concentration decreased during phase I but increased during phases II and III (Figure 3b), likely due to the additional carbon source provided by the added $NaHCO_3$. Throughout the experiment, the granule size of the sludge remained relatively stable, possibly due to the stirring conditions effectively mitigating sludge bulking and causing the granule size to approach a uniform size (Figure 3c). In summary, under stirring conditions, MBGS maintained the relative stability of the reaction system while adapting to and effectively treating wastewater following iron coagulation by altering algal metabolic activities and enhancing EPS secretion.

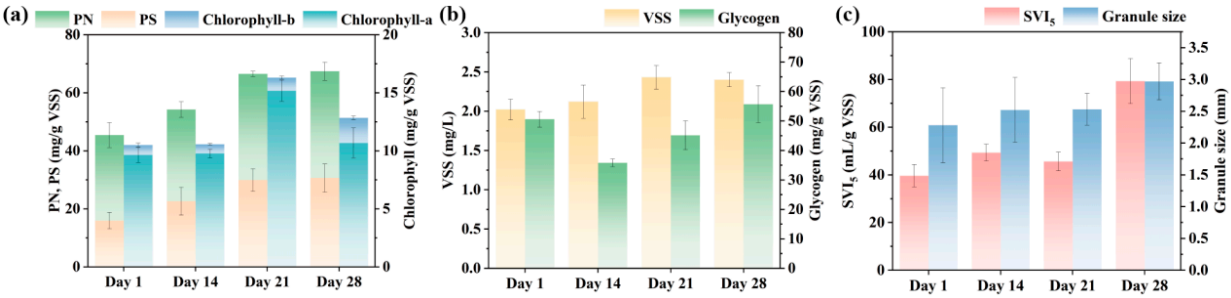


Figure 3. Characteristics of MBGS at different experimental phases: EPS and chlorophyll concentration (**a**); VSS and glycogen concentration (**b**); SVI_5 and granule size (**c**).

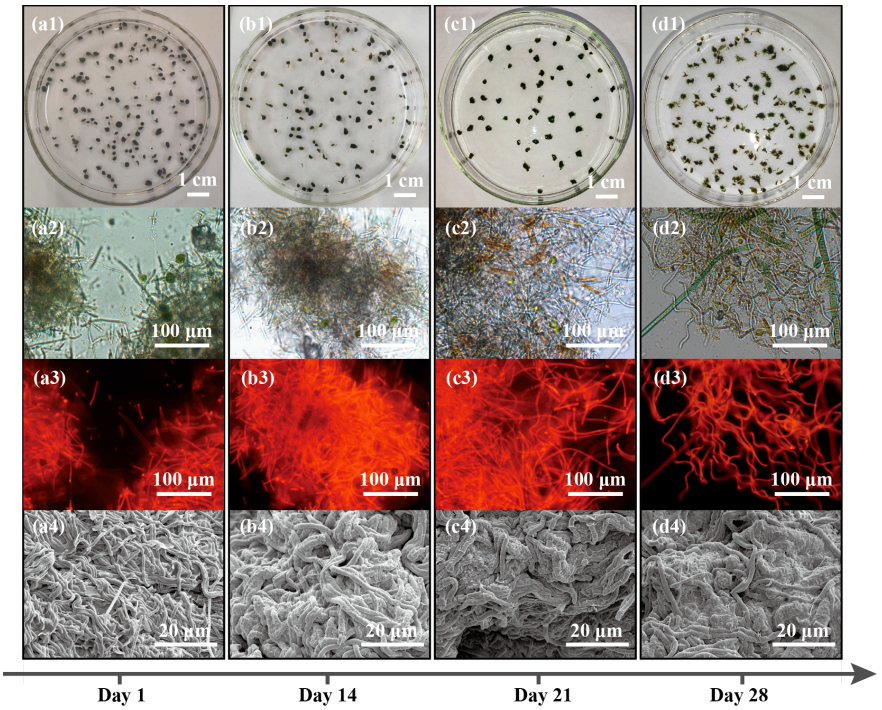


Figure 4. Images of MBGS observed using a camera (**a1**,**b1**,**c1**,**d1**), visible light microscopy (**a2**,**b2**,**c2**,**d2**), red fluorescence microscopy (**a3**,**b3**,**c3**,**d3**), and SEM (**a4**,**b4**,**c4**,**d4**).

3.4. Microbial Communities

As shown in Figure 5, throughout the experimental phases, the dominant phyla of prokaryotic microorganisms in MBGS were *Proteobacteria*, *Bacteroidota*, *Chloroflexi*, *Planc-*

tomycetota, and *Cyanobacteria*, while the dominant phyla of eukaryotic microorganisms were *Rotifera* and *Ciliophora*. These microorganisms played crucial roles in maintaining the stability of the MBGS system [27,28]. Among them, *Proteobacteria*, *Bacteroidota*, *Chloroflexi*, and *Planctomycetota*, as heterotrophic bacteria, were key functional microbes for the efficient removal of organic matter in the reactor. Compared to the early phases of the experiment, the relative abundance of *Cyanobacteria* increased by 23.5% on day 21. This increase was likely due to their effective utilization of the added inorganic carbon source for photosynthesis, which enhanced organic matter assimilation and supported their growth, thereby promoting TN removal [29]. However, by day 28, the relative abundance of *Cyanobacteria* decreased to 54.7% of that on day 21, likely due to the reduction in daytime light intensity, which hindered *Cyanobacteria* growth and their ability to continue effective photosynthesis (Table S1). The reduction in the abundance of *Cyanobacteria*—key microorganisms for maintaining the granular form of MBGS—may have contributed to the decreased settling performance of the sludge toward the end of the experiment. The reduction in the relative abundance of *Nitrospirae*, an important nitrite-oxidizing bacterium, early in the experiment might have negatively impacted nitrogen removal efficiency [30]. The decline in *Nitrospirae* abundance could have led to nitrite accumulation in the wastewater (see Figure S2), thereby reducing the overall nitrification efficiency and affecting total nitrogen removal and the conversion of ammonia to organic nitrogen. For eukaryotic microorganisms, the abundance of *Rotifera* significantly decreased toward the end of the experiment (Figure 5b). This decrease could be due to reduced metabolic rates, reproductive rates, and feeding activity in response to lower water temperatures. Notably, the total relative abundance of *Chlorophyta* and *Diatomea* increased significantly from day 21 to day 28 compared to the early phases of the experiment. This increase may be attributed to the effective absorption and accumulation of iron by *Chlorophyta* and *Diatomea*, thereby enhancing their utilization of other nutrients and improved their competitive advantage within the microbial community [24,25].

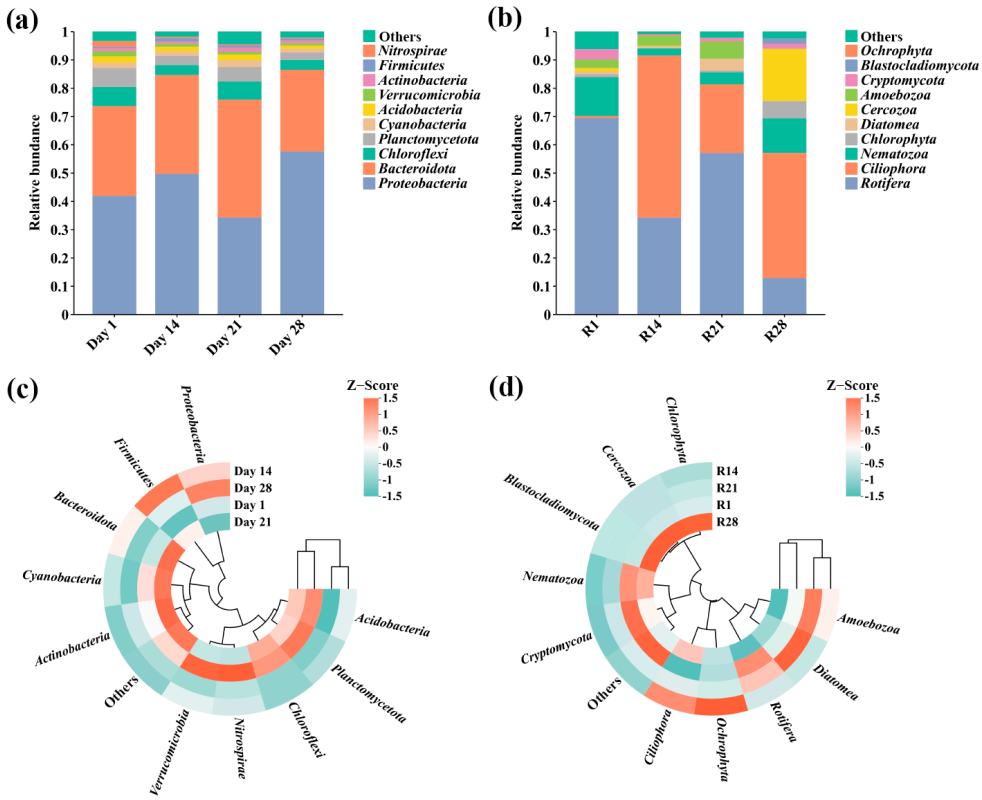


Figure 5. Changes in the relative abundance (**a**) and clustering relationships (**c**) of prokaryotic microorganisms, and the relative abundance (**b**) and clustering relationships (**d**) of eukaryotic microorganisms in MBGS system at different phases of the experiment.

3.5. Key Functional Genes

By investigating the key functional genes and gene abundance changes related to nitrogen, phosphorus, and organic matter removal in MBGS, it was observed that under parameter regulation, MBGS demonstrates excellent nitrogen fixation capability and adaptability to various carbon sources. As shown in Figure 6a, due to the absence of the key gene *NIT-6* in the assimilatory nitrate reduction process, nitrogen removal in MBGS primarily relies on dissimilatory nitrate reduction and denitrification processes [31]. It is important to note that nitrate predominantly originates from nitrification, as the influent contains almost no nitrite. In phase I of the experiment, the increased abundance of the functional gene *Hao*, responsible for hydroxylamine dehydrogenase synthesis, led to a rapid conversion of hydroxylamine to nitrite [32]. This increase in nitrite prompted a rise in the abundance of the *NxrAB* gene, which synthesizes nitrite oxidoreductase, facilitating the conversion of nitrite to nitrate. Further, the higher abundance of the functional genes *NarGHI* and *NapAB*, involved in nitrate reductase synthesis, promoted the reduction of nitrate to nitrite [33]. However, the low abundance of the genes *NirK*, *NirS*, *NorBC*, and *NosZ*, which are involved in synthesizing nitrite reductase, nitric oxide reductase, and nitrous oxide reductase during the subsequent denitrification process, may have hindered the further conversion of nitrite to nitrogen gas [34]. This is likely a reason for nitrite accumulation. In the later phases of the experiment (phases II to III), the reduced abundance of the key gene *NxrAB* weakened the conversion of nitrite to nitrate. Additionally, as the concentration of nitrate—the substrate for nitrate reductase—decreases, the abundance of the functional genes *NarGHI* and *NapAB* involved in nitrate reductase synthesis also declines, leading to reduced nitrite accumulation. The addition of $NaHCO_3$ enhanced algal photosynthesis, effectively reducing the competitive pressure on nitrogen-removal microorganisms for limited organic carbon. Toward the end of the experiment, although the abundance of the key gene *AmoCAB*, responsible for ammonia monooxygenase and crucial for nitrification, decreased, this was offset by the reduced nitrogen concentration in the influent and improved carbon-to-nitrogen ratio. Consequently, the activity of denitrifying bacteria was further enhanced, with the abundance of related functional genes (*NirK*, *NirS*, *NorBC*, and *NosZ*) increasing, which facilitated the conversion of nitrite to nitrogen gas.

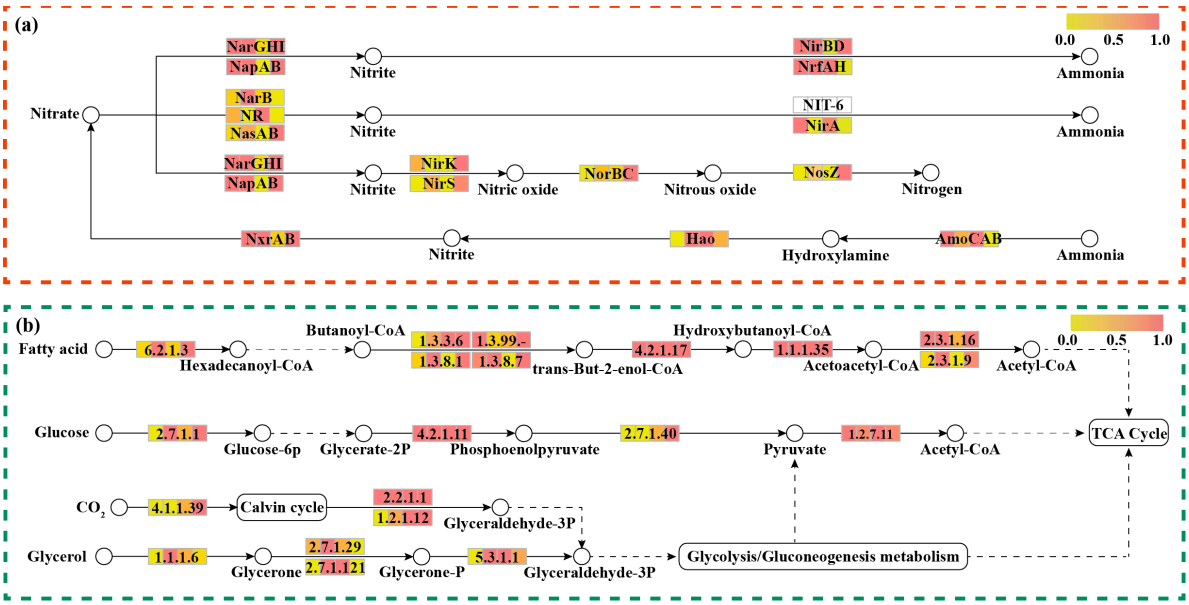


Figure 6. Main metabolic pathways and changes in the abundance of key functional genes for nutrient removal in MBGS during the experiment: nitrogen (**a**) and organic matter (**b**).

Since coagulation removes most colloids and particles, the energy sources for heterotrophic microorganisms in post-coagulation wastewater are primarily simple organic

compounds, such as fatty acids, glucose, and glycerol. The coding genes for enzymes involved in the initial steps of fatty acid, glucose, and glycerol metabolism (glycerol kinase, hexokinase, and glycerol-3-phosphate dehydrogenase; EC 6.2.1.3, EC 2.7.1.1, and EC 1.1.1.36, respectively) exhibited varying degrees of increased abundance throughout the experimental phases compared to the pre-experiment phase (Figure 6b). MBGS can utilize the aforementioned organic compounds for decomposition and metabolism to generate energy [21]. Additionally, the increased abundance of the coding gene for pyruvate carboxylase (EC 4.1.1.39) after the addition of $NaHCO_3$ suggested that pyruvate carboxylase assisted in converting CO_2 from the bicarbonate breakdown and pyruvate into oxaloacetate, which then participated in the Calvin cycle. This reflects the role of $NaHCO_3$ in supplementing carbon sources and enhancing pollutant removal in the MBGS process. The above indicates the excellent carbon fixation capability of MBGS and its adaptability to various types of carbon sources.

4. Conclusions

The wastewater treatment performance of the iron coagulation–MBGS coupling process was evaluated. The results indicated that the coagulation effect was optimal when the concentrations of Fe and PAM were 25 mg/L and 1 mg/L. MBGS can adapt to and accumulate residual iron in coagulated water by increasing EPS secretion and enhancing the abundance of eukaryotic algae. Due to the removal of large and recalcitrant organic particles by the coagulation process, MBGS consistently achieved high COD removal efficiencies of 81.1% (day) and 71.3% (night) combined with the contributions of heterotrophic microorganisms, such as *Proteobacteria*, *Bacteroidota*, and *Rotifera*. The addition of the inorganic carbon source $NaHCO_3$ addressed an issue of insufficient organic carbon, reduced nitrite accumulation, and enhanced denitrification, thereby improving nitrogen removal performance. Overall, through strategic parameter adjustments, MBGS can gradually adapt to iron-coagulated wastewater and exhibit performance that meets discharge standards. This study is expected to provide insights into the practical engineering applications of MBGS for realizing carbon-neutral wastewater treatment.

Supplementary Materials: The following supporting information can be downloaded at: https://www.mdpi.com/article/10.3390/w16213035/s1, Figure S1: Effects of coagulant (FeCl3) at different concentrations on COD, TN, and TP removal rates (a), turbidity, and pH (b); Effects of coagulant aids (PAM) at different concentrations on COD, TN, and TP removal rates (a), turbidity, and pH (b) after coagulant addition.; Figure S2: The day and night removal efficiencies and concentrations of ammonia and nitrite during the iron coagulation−MBGS coupling process; Table S1: Average light intensity, water temperature, and DO during the operation of the reactor.

Author Contributions: Investigation, Writing—original draft, Software, Formal analysis, B.C.; Investigation, Data curation, C.W.; Investigation, Data curation, C.C.; Conceptualization, A.L.; Writing—review and editing, X.Z., S.W. and B.J.; Funding acquisition, B.J. All authors have read and agreed to the published version of the manuscript.

Funding: This experiment was funded by the National Natural Science Foundation of China (52261135627; 52270048).

Data Availability Statement: Experimental data can be provided as required.

Conflicts of Interest: The authors declare that they have no known competing financial interests or personal relationships that could have appeared to influence the work reported in this paper.

References

1. Stasinakis, A.S.; Charalambous, P.; Vyrides, I. Dairy wastewater management in EU: Produced amounts, existing legislation, applied treatment processes and future challenges. *J. Environ. Manag.* **2022**, *303*, 114152. [CrossRef] [PubMed]
2. Yeoh, J.X.; Jamil, M.S.N.A.; Syukri, F.; Koyama, M.; Nourouzi Mobarekeh, M. Comparison between Conventional Treatment Processes and Advanced Oxidation Processes in Treating Slaughterhouse Wastewater: A Review. *Water* **2022**, *14*, 3778. [CrossRef]
3. Pervez, M.N.; Mishu, M.R.; Stylios, G.K.; Hasan, S.W.; Zhao, Y.; Cai, Y.; Zarra, T.; Belgiorno, V.; Naddeo, V. Sustainable Treatment of Food Industry Wastewater Using Membrane Technology: A Short Review. *Water* **2021**, *13*, 3450. [CrossRef]

4. Afolalu, S.A.; Ikumapayi, O.M.; Ogedengbe, T.S.; Kazeem, R.A.; Ogundipe, A.T. Waste pollution, wastewater and effluent treatment methods—An overview. *Mater. Today Proc.* **2022**, *62*, 3282–3288. [CrossRef]
5. Skouteris, G.; Rodriguez-Garcia, G.; Reinecke, S.F.; Hampel, U. The use of pure oxygen for aeration in aerobic wastewater treatment: A review of its potential and limitations. *Bioresour. Technol.* **2020**, *312*, 123595. [CrossRef]
6. Wilén, B.; Lumley, D.; Mattsson, A.; Mino, T. Relationship between floc composition and flocculation and settling properties studied at a full scale activated sludge plant. *Water Res.* **2008**, *42*, 4404–4418. [CrossRef]
7. Ahmed, M.B.; Zhou, J.L.; Ngo, H.H.; Guo, W.; Thomaidis, N.S.; Xu, J. Progress in the biological and chemical treatment technologies for emerging contaminant removal from wastewater: A critical review. *J. Hazard. Mater.* **2017**, *323*, 274–298. [CrossRef]
8. Teh, C.Y.; Budiman, P.M.; Shak, K.P.Y.; Wu, T.Y. Recent Advancement of Coagulation–Flocculation and Its Application in Wastewater Treatment. *Ind. Eng. Chem. Res.* **2016**, *55*, 4363–4389. [CrossRef]
9. Philips, S. Impact of iron salts on activated sludge and interaction with nitrite or nitrate. *Bioresour. Technol.* **2003**, *88*, 229–239. [CrossRef]
10. Ji, B.; Zhang, M.; Gu, J.; Ma, Y.; Liu, Y. A self-sustaining synergetic microalgal-bacterial granular sludge process towards energy-efficient and environmentally sustainable municipal wastewater treatment. *Water Res.* **2020**, *179*, 115884. [CrossRef]
11. Ameri, A.; Tamjidi, S.; Dehghankhalili, F.; Farhadi, A.; Saati, M.A. Application of algae as low cost and effective bio-adsorbent for removal of heavy metals from wastewater: A review study. *Environ. Technol. Rev.* **2020**, *9*, 85–110. [CrossRef]
12. Tang, C.; Hu, Y.; He, Z.; Li, Z.; Tian, Y.; Wang, X.C. Promoting symbiotic relationship between microalgae and bacteria in wastewater treatment processes: Technic comparison, microbial analysis, and future perspectives. *Chem. Eng. J.* **2024**, *498*, 155703. [CrossRef]
13. Sun, Y.; Chang, H.; Zhang, C.; Xie, Y.; Ho, S.H. Emerging biological wastewater treatment using microalgal-bacterial granules: A review. *Bioresour. Technol.* **2022**, *351*, 127089. [CrossRef] [PubMed]
14. Li, R.; Guo, X.; Li, B.; Lin, L.; Li, P.; Wen, L.; Liang, J.; Li, X. Iron-enhanced primary sedimentation and acidogenic sludge fermentation to achieve self-sufficient organic carbon supply for enhanced nutrient removal in wastewater treatment☆. *Resour. Conserv. Recycl.* **2021**, *164*, 105220. [CrossRef]
15. Xiao, Y.; Shen, Y.; Ji, B. Cultivation of microalgal-bacterial granular sludge from activated sludge via granule inoculation: Performance and microbial community. *J. Clean. Prod.* **2022**, *380*, 134875. [CrossRef]
16. Liu, H.; Zhou, Y.; Xiao, W.; Ji, L.; Cao, X.; Song, C. Shifting nutrient-mediated interactions between algae and bacteria in a microcosm: Evidence from alkaline phosphatase assay. *Microbiol. Res.* **2012**, *167*, 292–298. [CrossRef]
17. Zhang, W.; Cao, B.; Wang, D.; Ma, T.; Xia, H.; Yu, D. Influence of wastewater sludge treatment using combined peroxyacetic acid oxidation and inorganic coagulants re-flocculation on characteristics of extracellular polymeric substances (EPS). *Water Res.* **2016**, *88*, 728–739. [CrossRef]
18. Zhang, L.; Yang, G.; Hasan, H.A.; Fan, J.; Ji, B. Adaptation mechanisms of microalgal-bacterial granular sludge to outdoor light-limited conditions. *Environ. Res.* **2023**, *239*, 117244. [CrossRef]
19. Aguilar, M.I.; Sáez, J.; Lloréns, M.; Soler, A.; Ortuño, J.F.; Meseguer, V.; Fuentes, A. Improvement of coagulation–flocculation process using anionic polyacrylamide as coagulant aid. *Chemosphere* **2005**, *58*, 47–56. [CrossRef]
20. Bernat, K.; Wojnowska-Baryła, I. Carbon source in aerobic denitrification. *Biochem. Eng. J.* **2007**, *36*, 116–122. [CrossRef]
21. Peng, Y.; Zhu, G. Biological nitrogen removal with nitrification and denitrification via nitrite pathway. *Appl. Microbiol. Biotechnol.* **2006**, *73*, 15–26. [CrossRef] [PubMed]
22. Wang, Y.; Sun, P.; Lin, M.; He, Q.; Ji, B. Using Natural and Artificial Microalgal-Bacterial Granular Sludge for Wastewater Effluent Polishing. *Water* **2023**, *15*, 2605. [CrossRef]
23. Wang, H.; Qi, H.; Du, K.; Ran, D.; Liu, W.; Shen, X.; Zeng, R.J. Reinterpretation of the mechanism of coagulation and its effects in waste activated sludge treatment. *Sep. Purif. Technol.* **2022**, *291*, 120958. [CrossRef]
24. Norman, L.; Worms, I.A.M.; Angles, E.; Bowie, A.R.; Nichols, C.M.; Ninh Pham, A.; Slaveykova, V.I.; Townsend, A.T.; David Waite, T.; Hassler, C.S. The role of bacterial and algal exopolymeric substances in iron chemistry. *Mar. Chem.* **2015**, *173*, 148–161. [CrossRef]
25. Yuan, Y.; Jiang, M.; Zhu, X.; Yu, H.; Otte, M.L. Interactions between Fe and light strongly affect phytoplankton communities in a eutrophic lake. *Ecol. Indic.* **2021**, *126*, 107664. [CrossRef]
26. Roychoudhury, P.; Bose, R.; Dąbek, P.; Witkowski, A. Photonic Nano-/Microstructured Diatom Based Biosilica in Metal Modification and Removal—A Review. *Materials* **2022**, *15*, 6597. [CrossRef]
27. Ji, B.; Wang, S.; Silva, M.R.U.; Zhang, M.; Liu, Y. Microalgal-bacterial granular sludge for municipal wastewater treatment under simulated natural diel cycles: Performances-metabolic pathways-microbial community nexus. *Algal Res.* **2021**, *54*, 102198. [CrossRef]
28. Zhang, M.; Wang, Y.; Fan, Y.; Liu, Y.; Yu, M.; He, C.; Wu, J. Bioaugmentation of low C/N ratio wastewater: Effect of acetate and propionate on nutrient removal, substrate transformation, and microbial community behavior. *Bioresour. Technol.* **2020**, *306*, 122465. [CrossRef]
29. Cuellar-Bermudez, S.P.; Aleman-Nava, G.S.; Chandra, R.; Garcia-Perez, J.S.; Contreras-Angulo, J.R.; Markou, G.; Muylaert, K.; Rittmann, B.E.; Parra-Saldivar, R. Nutrients utilization and contaminants removal. A review of two approaches of algae and cyanobacteria in wastewater. *Algal Res.* **2017**, *24*, 438–449. [CrossRef]

30. Mehrani, M.; Sobotka, D.; Kowal, P.; Ciesielski, S.; Makinia, J. The occurrence and role of Nitrospira in nitrogen removal systems. *Bioresour. Technol.* **2020**, *303*, 122936. [CrossRef]
31. Besson, S.; Almeida, M.G.; Silveira, C.M. Nitrite reduction in bacteria: A comprehensive view of nitrite reductases. *Coord. Chem. Rev.* **2022**, *464*, 214560. [CrossRef]
32. Huang, W.; Gong, B.; Wang, Y.; Lin, Z.; He, L.; Zhou, J.; He, Q. Metagenomic analysis reveals enhanced nutrients removal from low C/N municipal wastewater in a pilot-scale modified AAO system coupling electrolysis. *Water Res.* **2020**, *173*, 115530. [CrossRef] [PubMed]
33. Huang, S.; Zhang, B.; Zhao, Z.; Yang, C.; Zhang, B.; Cui, F.; Lens, P.N.L.; Shi, W. Metagenomic analysis reveals the responses of microbial communities and nitrogen metabolic pathways to polystyrene micro(nano)plastics in activated sludge systems. *Water Res.* **2023**, *241*, 120161. [CrossRef] [PubMed]
34. Feng, L.; Yang, J.; Yu, H.; Lan, Z.; Ye, X.; Yang, G.; Yang, Q.; Zhou, J. Response of denitrifying community, denitrification genes and antibiotic resistance genes to oxytetracycline stress in polycaprolactone supported solid-phase denitrification reactor. *Bioresour. Technol.* **2020**, *308*, 123274. [CrossRef]

Disclaimer/Publisher's Note: The statements, opinions and data contained in all publications are solely those of the individual author(s) and contributor(s) and not of MDPI and/or the editor(s). MDPI and/or the editor(s) disclaim responsibility for any injury to people or property resulting from any ideas, methods, instructions or products referred to in the content.